Chinese Chemical Letters 37 (2026) 111930

Contents lists available at ScienceDirect

Chinese Chemical Letters

journal homepage: www.elsevier.com/locate/cclet

Oligomeric α-diimine nickel catalysts for enhanced ethylene polymerization

Jingfeng Yue [a,b], Zhenxin Tang [a], Yuxing Zhang [a,*], Zhongbao Jian [a,b,*]

[a] State Key Laboratory of Polymer Science and Technology, Changchun Institute of Applied Chemistry, Chinese Academy of Sciences, Changchun 130022, China

[b] School of Applied Chemistry and Engineering, University of Science and Technology of China, Hefei 230026, China

ARTICLE INFO

Article history:
Received 10 July 2025
Revised 23 September 2025
Accepted 29 September 2025
Available online 30 September 2025

Keywords:
Polyolefin
Oligomeric catalyst
Polyethylene elastomer
Ethylene polymerization
Nickel catalyst

ABSTRACT

Catalysts are key for olefin polymerization reactions and are also ubiquitous in catalysis science. Multi-nuclear metal catalysts have witnessed enhanced performances in catalytic reactions relative to mono-nuclear catalysts, but which substantially involve multi-step, tedious, and difficult synthesis. Herein, this study reports an intriguing approach to construct multi-nuclear catalysts for the milestone α-diimine nickel catalysts using an oligomeric strategy. A polymerizable norbornene unit is incorporated into the α-diimine ligand backbone, leading to the formation of the monomeric nickel catalyst Ni_1 and its corresponding oligomeric nickel catalysts (Ni_3 and Ni_5) with varying degrees of polymerization (DP = 3 and 5). Notably, the oligomeric catalyst Ni_5 was facilely scaled up (50 g-level), showed enhanced thermal stability, exhibited 4.6 times higher activity, and yielded polyethylene elastomer with a 379 % increased molecular weight in ethylene polymerization, compared to the monomeric catalyst Ni_1. Catalytic performance enhancements of oligomeric catalysts were found to be DP-dependent. The kilogram-scale polyethylene, produced using Ni_5 in a 20 L reactor, presented a highly branched all-hydrocarbon structure, which demonstrated typical elastic properties (tensile strength: 4 MPa, elastic recovery: SR = 72 %) along with great processability (MFI = 3.0 g/10 min), insulating characteristics (volume resistivity = 2×10^{16} Ω/m), and hydrophobicity (water vapor permeability: 0.03 g/m^2/day), suggesting potentially practical applications.

© 2025 Published by Elsevier B.V. on behalf of Chinese Chemical Society and Institute of Materia Medica, Chinese Academy of Medical Sciences.

The advancement of olefin polymerization technologies has been fundamentally driven by continuous innovations in organometallic catalysts. Following Ziegler and Natta's groundbreaking discovery of Ti-based catalysts in the 1950s, the field has witnessed successive generations of catalytic systems ranging from Phillips catalysts to metallocene catalysts and post-metallocene catalysts [1–7]. These breakthroughs in catalyst technology have notably propelled the development of the global polyolefin industry [8].

Olefin polymerization employs two principal methodologies: homogeneous solution processes and heterogeneous gas/slurry-phase systems (Fig. 1). Homogeneous catalysis, typically mediated by solvent-soluble molecular catalysts such as metallocenes, excels in producing low-crystallinity plastomers and elastomers [9,10]. This method is not optimal for semi-crystalline polyolefins such as high-density polyethylene (HDPE) and isotactic polypropylene (*i*PP), where these polymers are insoluble in the reaction medium. To prevent reactor fouling and ensure smooth operations, morphologically uniform polymer particles are required, thereby enabling a continuous process [11,12]. As such, it becomes pertinent to prepare immobilized catalysts by combining the catalyst with inorganic or organic supports, through covalent [13–15], ionic [16–20], or hydrogen bonding [21]. However, immobilization of catalysts often negatively affected their performance especially for catalytic activity [22,23]. Particularly for late transition metal catalysts (*e.g.*, α-diimine Ni(II) systems) that exhibit chain-walking behavior [24–37], immobilization on either silica or other inorganic support often suppresses the characteristic branching density, diminishing the unique elastomeric properties of resultant polyethylenes [38,39].

Recently, in terms of the important role of multi-nuclear catalysts in enhancing olefin polymerization, polymeric catalysts have garnered interest as an innovative catalyst design approach [40–46]. Unlike traditional multi-nuclear catalysts that always require multi-step, tedious, and difficult synthesis, polymeric catalysts offered a more straightforward synthesis, facilitating the transition from mono-nuclear to multi-nuclear catalyst through polymerizable groups such as the common unsaturated double bonds.

* Corresponding authors.
E-mail addresses: yxzhang7@ciac.ac.cn (Y. Zhang), zbjian@ciac.ac.cn (Z. Jian).

https://doi.org/10.1016/j.cclet.2025.111930
1001-8417/© 2025 Published by Elsevier B.V. on behalf of Chinese Chemical Society and Institute of Materia Medica, Chinese Academy of Medical Sciences.

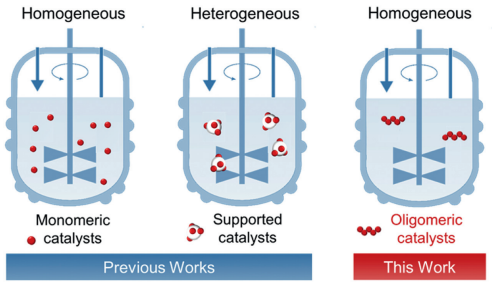


Fig. 1. Synopsis of olefin catalytic polymerization type. Homogeneous solution polymerization using monomeric catalysts, heterogeneous gas-phase or slurry-phase polymerization using supported catalysts (previous works), and oligomeric catalysts promoted homogeneous solution polymerization (this work).

Representative advances included poly(norbornene-*graft*-styrene)-supported Ti and Zr phenoxy-imine catalysts, demonstrating one order of magnitude higher activity over monomeric analogues in ethylene polymerization [47], and styrene-derived polymeric α-diimine Pd(II) catalysts, achieving improved tolerance to polar comonomers, leading to higher activities as well as higher molecular weights in ethylene–methyl acrylate copolymerization [46].

In this study, we report a strategy of oligomeric Ni(II) catalysts for chain walking ethylene polymerization. Through rational introduction of polymerizable norbornene moiety into the milestone α-diimine Ni(II) catalyst, we achieved a control over catalyst oligomerization *via* ring-opening metathesis polymerization (ROMP) (Fig. 2a). Through the control of the degree of polymerization (DP) of the oligomeric catalysts, two highly active Ni(II) catalysts were prepared. Notably, compared to their monomeric nickel counterpart, the oligomeric variants exhibited remarkable improvements in both catalytic activity and polymer molecular weight. By using a 20 L polymerization reactor, a kilogram scale of polyethylene (PE) elastomer was successfully produced in an activity level of 10^7 g mol^{-1} h^{-1}. Notably, these polyethylenes were highly branched and showcased amorphous properties and excellent transparency: hallmark attributes of elastomers.

The synthetic route for the oligomeric nickel catalysts for chain walking olefin polymerization in this study was delineated in Fig. 2a. The polymerizable ligand was designed by installing a ring-opening metathesis polymerization (ROMP) type cyclic olefin unit into the α-diimine ligand, which was synthesized by the reaction of a norbornene-modified diketone [48] and 2,6-diisopropyl aniline (detailed synthetic procedures and characterizations were provided in Supporting information). Subsequent coordination of the ligand with stoichiometric $NiBr_2$(DME) (DME = 1,2-dimethoxyethane) yielded the monomeric catalyst Ni_1 (Fig. 2b). Oligomerization of Ni_1 was then achieved *via* G2 (the 2nd generation Grubbs catalyst) mediated ROMP, producing well-defined oligomeric catalysts Ni_3 and Ni_5 with degrees of polymerization (DP) of 3 and 5, respectively. Compared with conventional multi-nuclear catalysts that require sophisticated structural design and intricate synthesis procedures, the strategy of oligomeric nickel catalysts offered a more efficient synthesis process to construct a multi-nuclear structure. For instance, the production of Ni_5 can be efficiently scaled up to 50 g in a laboratory (Supporting information).

Comprehensive structural characterization of the ligand and catalysts was performed using NMR (nuclear magnetic resonance) spectroscopy, MS (mass spectrometry), and elemental analysis (Supporting information). A distinct chromatic evolution was observed among these ligand and catalysts: Solutions transitioned progressively from yellow (free ligand) to orange (monomeric Ni_1), and ultimately to deep red/maroon for oligomeric Ni_3 and Ni_5 (Fig. 2c). This transition was correlated with characteristic UV–vis spectral changes (Fig. 2d), where an absorption peak emerged at 540 nm from the ligand to Ni_1. This peak corresponded to green light, resulting in a shift in the solution's color from yellow to orange, which can be attributed to the pronounced metal-to-ligand charge transfer (MLCT) absorptions in the visible range of 500–600 nm [49]. Both Ni_3 and Ni_5 exhibited absorption within this range with heightened intensity, in which Ni_5 with the higher DP demonstrated the most intense absorption, accounting for the gradual deepening of the solution color.

Under the activation of methylaluminoxane (MAO), Ni_1, Ni_3, and Ni_5 were employed in ethylene polymerization (Table 1). In general, the catalytic performance of these three catalysts demonstrated similar trends across varying reaction conditions, producing highly branched PE (Fig. 3). As the reaction temperature increased from 30 °C to 90 °C, a decrease in both catalytic activity and polymer molecular weight was observed, along with an increase in polymer branching density. These observations were consistent with previous reports [14]. Higher temperatures could cause partial deactivation of the catalyst and lower solubility of ethylene. The former reduced the active species, while the latter led to a slower chain growth rate. Both factors contributed to a decrease in catalytic activity. The reduction in polymer molecular weight and increase in branching density can be attributed to a higher propensity for β-H elimination at a higher temperature, thereby accelerating chain transfer and chain walking [50,51]. As ethylene pressure elevated from 1 bar to 4 bar and 8 bar, both catalytic activity and polymer molecular weight were enhanced (Table 1, entries 11, 13 and 14). Concurrently, the polymer branching density witnessed a

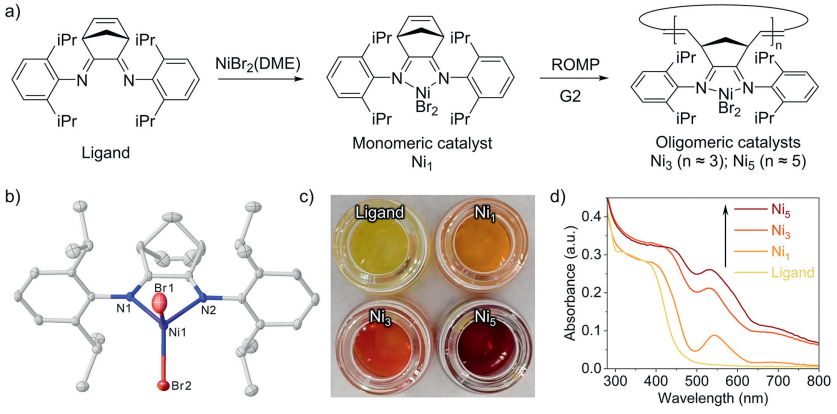


Fig. 2. (a) Synthetic route of monomeric catalyst Ni_1 and subsequent oligomerization *via* ROMP to yield the corresponding oligomeric catalysts Ni_3 (DP ≈ 3) and Ni_5 (DP ≈ 5). (b) Solid-state structure of Ni_1. (c) CH_2Cl_2 solutions of ligand and Ni_1, Ni_3, Ni_5 at a concentration of 9×10^{-3} mol/L. (d) UV–vis spectroscopy of the four solutions in (c) with 1 cm optical path.

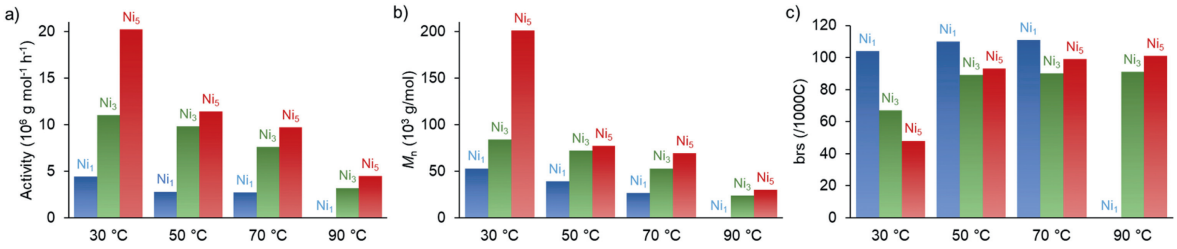


Fig. 3. Comparison of ethylene polymerization activated by MAO between monomeric Ni_1 and oligomeric Ni_3 and Ni_5 in terms of (a) activity, (b) polymer molecular weight, and (c) branching density.

Table 1
Effect of temperature on ethylene polymerization with Ni(II) catalysts.[a]

Entry	Cat.	T (°C)	P (bar)	Yield (g)	Act. (10^6)[b]	M_n (kDa)[c]	M_w/M_n[c]	brs[d]
1	Ni_1	30	8	2.2	4.4	53.0	2.65	104
2	Ni_1	50	8	1.4	2.8	39.2	2.57	110
3	Ni_1	70	8	1.3	2.7	26.5	2.92	111
4	Ni_1	90	8	trace	–	–	–	–
5	Ni_3	30	8	5.5	11.0	83.8	2.67	67
6	Ni_3	50	8	4.9	9.8	72.0	2.86	89
7	Ni_3	70	8	3.8	7.6	53.0	2.10	90
8	Ni_3	90	8	1.6	3.2	23.5	1.94	91
9	Ni_5	30	8	10.1	20.2	201	2.43	48
10	Ni_5	50	8	5.7	11.4	77.4	2.56	93
11	Ni_5	70	8	4.9	9.7	69.3	2.67	99
12	Ni_5	90	8	2.2	4.5	30.2	1.95	101
13	Ni_5	70	1	1.2	2.4	28.7	2.21	116
14	Ni_5	70	4	2.4	4.8	32.1	1.99	115

[a] Reaction conditions: Nickel molar number in catalyst (1 μmol), MAO (500 equiv.), toluene/CH_2Cl_2 (98/2 mL), polymerization time (30 min), unless noted otherwise.
[b] Activity is in unit of g mol^{-1} h^{-1}.
[c] Determined by GPC in 1,2,4-trichlorobenzene at 150 °C using a light scattering detector.
[d] brs = Number of branches per 1000C, as determined by ^{1}H NMR spectroscopy.

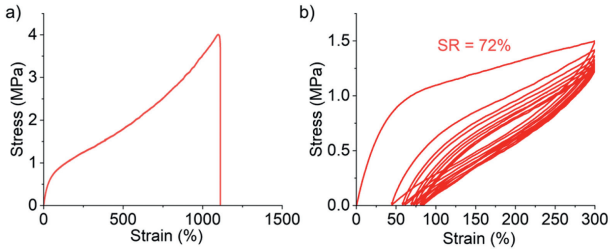


Fig. 4. Stress-strain curve and plots of hysteresis experiments of (a) ten cycles at a strain of 300 % and (b) for the highly branched polyethylene sample (Table S1, entry 9).

gradual decline. This can be attributed to the rise in ethylene concentration, which resulted in an accelerated chain growth rate [52]. Notably, replacing toluene with industrially favorable hexane (Table S4 in Supporting information) resulted in comparable polymer molecular weights but enhanced catalytic activity.

It is noteworthy that oligomeric catalysts Ni_3 and Ni_5 demonstrated remarkable enhancement in catalytic performance relative to the monomeric catalyst Ni_1 in terms of thermostability, catalytic activity, and polymer molecular weight (Fig. 3). Under identical reaction conditions, Ni_5 significantly outperformed Ni_3 and Ni_1 in both catalytic activity and polymer molecular weight (Figs. 3a and b). At 30 °C, Ni_5 exhibited 4.6-fold higher activity (20.2×10^6 *vs.* 4.4×10^6 g mol^{-1} h^{-1}) and 3.8-fold greater polymer molecular weight (201 *vs.* 53 kDa) than Ni_1 (Table 1, entry 9 *vs.* 1). Even at 90 °C, Ni_3 and Ni_5 retained substantial activities (3.2×10^6 and 4.5×10^6 g mol^{-1} h^{-1}, respectively), while Ni_1 was complete deactivation. The enhanced catalytic performance scaled with the increase of the DP of oligomeric catalysts, as Ni_5 (DP ≈ 5) consistently surpassed Ni_3 (DP ≈ 3) across all tested conditions, indicating a DP-dependent feature (Table 1, entries 5–12). In addition, the polymer branching densities of PE produced by multi-nuclear catalysts (Ni_3 and Ni_5) were found to be lower than that produced by the monomeric Ni_1. This could be attributed to the increased steric hindrance surrounding the metal centers due to the formation of multi-nuclear architectures, which effectively reduced β-H elimination and chain-walking, thus resulting in a decreased branching density.

Ethylene polymerization using Ni_1, Ni_3, and Ni_5 activated by diethyl aluminum chloride (Et_2AlCl) was also systematically investigated in parallel with MAO (Table S1 and Fig. S1 in Supporting information). Polymerization results showed that Ni_1, Ni_3, and Ni_5 catalysts exhibited up to 2-fold enhanced activities (22.8×10^6 *vs.* 11.4×10^6 g mol^{-1} h^{-1}) when activated by Et_2AlCl compared to MAO (Table S1, entry 10 *vs.* Table 1, entry 10), while demonstrated a reduction in polymer molecular weights (M_w = 77.4 kDa *vs.* 49.9 kDa). Notably, both catalytic systems displayed analogous temperature- and structure-dependent trends, with oligomeric Ni_3 and Ni_5 demonstrating superior performance in both activity and polymer molecular weight compared to the monomeric Ni_1 catalyst (Fig. 3 and Fig. S1). This consistent behavior over different activator underscored the advantage of oligomeric catalyst in ethylene polymerization. The synthesized highly branched polyethylene displayed properties akin to conventional elastomers. An exemplary sample (Table S1, entry 9; brs = 72/1000C) achieved a tensile strength of 4.0 MPa with 1100 % of elongation at break, exhibiting typically elastic recovery of 72 % (Fig. 4). In contrast, samples with a lower branching density (Table 1, entry 9; brs = 48/1000C) exhibited enhanced tensile strength (23.8 MPa, Fig. S54 in Supporting information). Moreover, the polymer branching density also influenced materials density (Table S3 in Supporting information). Specifically, the less branched sample (Table 1, entry 9) exhibited a higher density (0.890 g/cm^3) compared to its highly branched counterpart (Table S1, entry 9; 0.879 g/cm^3).

Scale-up experiments conducted in a 20 L high-pressure reactor (20 bar of ethylene pressure) at hexane confirmed the potentially industrial viability of oligomeric catalysts (Fig. 5). Ni_5 achieved remarkable productivity of 10^7 g mol^{-1} h^{-1} (approximately 15 kg_{PE}/g_{Cat}), producing 1 kg of branched polyethylene with moderate molecular weight (M_w = 91.1 kDa) and excellent melt processability (melt flow index, MFI = 3.0 g/10 min at 190 °C/2.16 kg). This significantly outperformed the sample from Table 1, entry 9 (MFI = 0.023 g/10 min) with higher molecular weight of M_w = 488 kDa. Notably, Ni_5 demonstrated consistent activities over five repeated polymerizations, suggesting an outstanding repeatability (Fig. 5b). In contrast, the monomeric Ni_1 exhibited significantly lower activity (2.4×10^6 g mol^{-1} h^{-1}, approximately 3.6 kg_{PE}/g_{Cat}) and molecular weight (M_w = 14.7 kDa) under identical conditions, as detailed in Table 2.

1 kg of polyethylene prepared by Ni_5 in a 20 L reactor exhibited highly branched architecture with a complicated branching

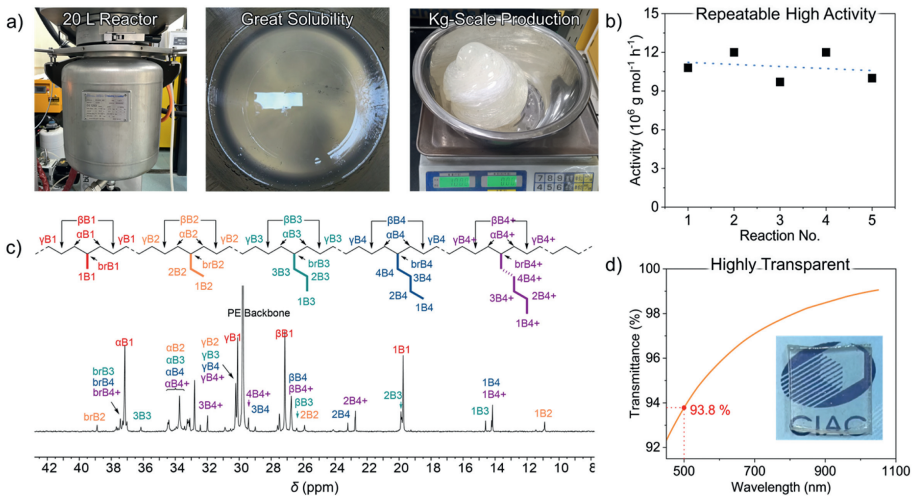


Fig. 5. (a) Kilogram-scale of highly branched PE produced *via* a 20 L reactor. (b) Scale-up ethylene polymerizations using Ni_5 was repeated for 5 times (Table S2 in Supporting information). (c) ^{13}C NMR spectrum ($CDCl_3$, 25 °C) of branched PE (Table 2, entry 2). (d) Optical properties of highly branched PE produced in a 20 L reactor (Table 2, entry 2).

Table 2
Ethylene polymerization using Ni_1 and Ni_5 in a 20 L reactor.[a]

Entry	Cat.	Yield (g)	Act. (10^6) [b]	M_w (kDa) [c]	M_w/M_n [c]	brs [d]	T_m (°C)[e]
1	Ni_1	~240	~2.4	14.7	2.78	78	/
2	Ni_5	~1000	~10.0	91.1	1.86	82	46

[a] Reaction conditions: Nickel molar number in catalyst (100 μmol), MAO (500 equiv.), hexane (13 L), ethylene pressure (20 bar), polymerization time (1 h), temperature (~65 °C), unless noted otherwise.
[b] Activity is in unit of g mol^{-1} h^{-1}.
[c] Determined by GPC in 1,2,4-trichlorobenzene at 150 °C using a light scattering detector.
[d] brs = Number of branches per 1000C, as determined by ^1H NMR spectroscopy.
[e] Determined by DSC (second heating).

pattern, including methyl (B1), ethyl (B2), propyl (B3), butyl (B4) and longer branches (B4+) (Fig. 5c). ^{13}C NMR [53] spectrum revealed that methyl branching at 19.88 ppm was the most branching pattern, contributing up to 70 % of the content, followed by longer branches than butyl (B4+, 14.30 ppm) with a content of 13 %. This high branching structure endowed the PE with notable properties such as a low melting point (46 °C), low density (0.850 g/cm^3), excellent ductility (Fig. S54), good solubility, and high transparency due to reduced crystallinity. In detail, the highly branched PE could fully dissolve in the reaction solvent (hexane) without any precipitation, yielding a clear, transparent, and highly viscous solution with polymer content up to 10.4 wt% after polymerization (Fig. 5a). Also, the polymer film exhibited high transparency, with a transmittance reaching 93.8 % at 500 nm (sample thickness: 0.17 mm) (Fig. 5d). This all-hydrocarbon structure endowed such highly branched polyethylene with good insulation properties, achieving a volume resistivity of 2×10^{16} Ω/m. Coupled with hydrophobicity, it exhibited a water vapor permeability of 0.03 g/m^2/day, comparable with commercial polyolefin elastomer (Table S3), suggesting potentially practical applications.

In summary, this work presented an oligomeric approach for α-diimine nickel catalyst design, which advances the conventional mono-nuclear nickel catalysts and reforms the multi-nuclear nickel catalysts using a complicated synthesis. By incorporating norbornene-modified ligands followed by ring-opening metathesis polymerization, oligomeric nickel catalysts with varied degree of polymerization (DP) were constructed. Comprehensive evaluation revealed that the oligomeric catalyst strategy significantly governed catalytic performance enhancements: Ni_5 demonstrated 4.6-fold higher activity and produced polyethylene with 379 % increased molecular weight, relative to the monomeric counterpart Ni_1. Notably, these improvements were intensified as the DP of the oligomeric catalyst increased, indicating the effectiveness of the oligomeric catalyst strategy. The resultant highly branched polyethylenes exhibited remarkable elastic recovery (72 %), while kilogram-scale synthesis in a 20 L reactor indicated potentially industrial application. In contrast to previous modifications that have majorly relied on tedious ligand substituents, the oligomeric nickel catalyst described in this work has witnessed a key step to enhance the catalytic performance in olefin polymerization. This provides a new avenue for the development of late-transition metal catalysts and beyond. At present, we are working for new polyolefin catalysts by using this oligomeric catalyst strategy.

Declaration of competing interest

The authors declare that they have no known competing financial interests or personal relationships that could have appeared to influence the work reported in this paper.

CRediT authorship contribution statement

Jingfeng Yue: Methodology, Investigation, Formal analysis, Data curation. **Zhenxin Tang:** Investigation, Data curation. **Yuxing Zhang:** Writing – original draft, Project administration, Funding acquisition, Formal analysis, Conceptualization. **Zhongbao Jian:** Writing – review & editing, Supervision, Project administration, Conceptualization.

Acknowledgments

The authors are thankful for financial support from the National Natural Science Foundation of China (Nos. 22401274, U23B6011), and the Jilin Provincial Science and Technology Department Program (No. 20250102070JC).

Supplementary materials

Supplementary material associated with this article can be found, in the online version, at doi:10.1016/j.cclet.2025.111930.

References

[1] V.K. Soni, R. Rani, G. Singh, Eur. Polym. J. 226 (2025) 113741.
[2] M. Stürzel, S. Mihan, R. Mülhaupt, Chem. Rev. 116 (2016) 1398–1433.
[3] M.P. McDaniel, Adv. Catal. 53 (2010) 123–606.
[4] M.M. Stalzer, M. Delferro, T.J. Marks, Catal. Lett. 145 (2015) 3–14.
[5] C. Copéret, F. Allouche, K.W. Chan, Angew. Chem. Int. Ed. 57 (2018) 6398–6440.
[6] H. Makio, T. Fujita, Acc. Chem. Res. 42 (2009) 1532–1544.
[7] G. Zanchin, G. Leone, Prog. Polym. Sci. 113 (2021) 101342.
[8] R.M. Patel, P. Jain, B. Story, S. Chum, Polyethylene: an account of scientific discovery and industrial innovations, in: W.H. Flank, M.A. Abraham, M.A. Matthews (Eds.), Innovations in Industrial and Engineering Chemistry, American Chemical Society, 2008, pp. 71–102.
[9] P.S. Chum, K.W. Swogger, Prog. Polym. Sci. 33 (2008) 797–819.
[10] C. Wang, X. Li, S. Chen, T.Y. Shan, Materials 18 (2025) 1334.
[11] L.L. Böhm, Angew. Chem. Int. Ed. 42 (2003) 5010–5030.
[12] R.J. Witzke, A. Chapovetsky, M.P. Conley, D.M. Kaphan, M. Delferro, ACS Catal. 10 (2020) 11822–11840.
[13] J.R. Severn, J.C. Chadwick, R. Duchateau, N. Friederichs, Chem. Rev. 105 (2005) 4073–4147.
[14] Z.S. Ma, M.L. Xu, N.N. Zhu, C. Tan, C.L. Chen, Chin. J. Chem. 41 (2023) 1155–1162.
[15] H.S. Schrekker, V. Kotov, P. Preishuber-Pflugl, P. White, M. Brookhart, Macromolecules 39 (2006) 6341–6354.
[16] C.W. Hong, Z.H. Wang, H. Jiang, et al., Chin. Chem. Lett. 34 (2023) 107918.
[17] L.C. Simon, H. Patel, J.B.P. Soares, R.F. de Souza, Macromol. Chem. Phys. 202 (2001) 3237–3247.
[18] Q. Wang, Z. Zhang, C. Zou, C.L. Chen, Chin. Chem. Lett. 33 (2022) 4363–4366.
[19] M.R. Ribeiro, A. Deffieux, M.F. Portela, Ind. Eng. Chem. Res. 36 (1997) 1224–1237.
[20] Y. Choi, J.B.P. Soares, Macromol. Chem. Phys. 210 (2009) 1979–1988.
[21] H. Zhang, C. Zou, H.P. Zhao, Z.G. Cai, C.L. Chen, Angew. Chem. Int. Ed. 60 (2021) 17446–17451.
[22] R.B. Huang, R. Duchateau, C.E. Koning, J.C. Chadwick, Macromolecules 41 (2008) 579–590.
[23] R. Guimarães, F.C. Stedile, J.H.Z. dos Santos, J. Mol. Catal. A: Chem. 206 (2003) 353–362.
[24] L.K. Johnson, C.M. Killian, M. Brookhart, J. Am. Chem. Soc. 117 (1995) 6414–6415.
[25] L.K. Johnson, S. Mecking, M. Brookhart, J. Am. Chem. Soc. 118 (1996) 267–268.
[26] S. Mecking, L.K. Johnson, L. Wang, M. Brookhart, J. Am. Chem. Soc. 120 (1998) 888–899.
[27] X.Q. Hu, Y.X. Zhang, B. Li, Z.B. Jian, Chin. J. Chem. 39 (2021) 2829–2836.
[28] J.S. Yang, X.Q. Hu, Z.B. Jian, Chin. J. Chem. 40 (2022) 2919–2926.
[29] J.S. Yang, Y.X. Zhang, Z.B. Jian, Chem. Res. Chin. Univ. 39 (2023) 797–802.
[30] Y.X. Zhang, Y.X. Zhang, X.Q. Hu, Z.B. Jian, ACS Catal. 12 (2022) 14304–14320.
[31] R.Y. Yuan, Y.Z. Wang, Q. Mahmood, et al., Polymer 293 (2024) 126690.
[32] Y.T. Zheng, Q.C. Wang, Y.P. Che, et al., Eur. Polym. J. 203 (2024) 112649.
[33] Z. Lu, B.H. Ding, S.Y. Dai, Macromolecules 57 (2024) 5262–5270.
[34] Z. Lu, X.W. Xu, Y. Luo, et al., ACS Catal. 13 (2023) 725–734.
[35] H.D. Zheng, Y.W. Li, W.B. Du, et al., Macromolecules 55 (2022) 3533–3540.
[36] H.D. Zheng, Z.L. Qiu, H. Gao, et al., Macromolecules 57 (2024) 5279–5288.
[37] W.C. Anderson Jr., J.L. Rhinehart, A.G. Tennyson, B.K. Long, J. Am. Chem. Soc. 138 (2016) 774–777.
[38] P. Preishuber-Pflugl, M. Brookhart, Macromolecules 35 (2002) 6074–6076.
[39] R.K. Wu, T.M. Lenz, L. Stieglitz, et al., J. Catal. 426 (2023) 270–282.
[40] M. Delferro, T.J. Marks, Chem. Rev. 111 (2011) 2450–2485.
[41] B. Heurtefeu, C. Bouilhac, É. Cloutet, D. Taton, A. Deffieux, H. Cramail, Prog. Polym. Sci. 36 (2011) 89–126.
[42] D. Peng, M.H. Xu, C. Tan, C.L. Chen, Macromolecules 56 (2023) 2388–2396.
[43] R.Y. Zhang, S.J. Liu, C.W. Zhuo, H. Cao, X.H. Wang, Macromolecules 57 (2023) 132–141.
[44] Z.Z. Zhou, S.J. Liu, L.H. Yang, et al., ACS Catal. 13 (2023) 15116–15125.
[45] L.H. Yang, S.J. Liu, Z.Z. Zhou, et al., Macromolecules 57 (2023) 150–161.
[46] M.H. Ji, G.F. Si, Y. Pan, C. Tan, M. Chen, J. Catal. 415 (2022) 51–57.
[47] Z. Dong, W.J. Huang, X.Q. Liu, et al., Macromolecules 54 (2021) 9385–9392.
[48] J.A. Molina de la Torre, A.C. Albéniz, Eur. J. Inorg. Chem. 22 (2017) 2911–2919.
[49] C. Sondermann, M. Pižl, A. Paretzki, C. Feil, et al., Eur. J. Inorg. Chem. 31 (2020) 3010–3015.
[50] S.A. Svejda, L.K. Johnson, M. Brookhart, J. Am. Chem. Soc. 121 (1999) 10634–10635.
[51] Y.X. Zhang, X.H. Kang, Z.B. Jian, Nat. Commun. 13 (2022) 725.
[52] J. Xia, Y.X. Zhang, S.Q. Kou, Z.B. Jian, J. Catal. 390 (2020) 30–36.
[53] H.Y. Ji, Y.X. Zhang, Y. Chi, Z.B. Jian, Polymer 290 (2024) 126591.